Estimation of the Location of a Scatterer from Interferometric Ghosts of the Scattered Surface Waves

U. Harmankaya[1], A. Kaslilar[1], J.Thorbecke[2], K.Wapenaar[2] and D. Draganov[2]*

[1]Istanbul Technical University
[2]Delft University of Technology

Summary

In this study, we use the interferometric ghosts of the scattered surface waves for estimating the location of a near-surface scatterer. The scatterer is embedded in a homogeneous halfspace. We perform finite difference modeling of elastic wave propagation to calculate the seismograms. We choose different locations for virtual sources and obtain interferometric estimates of the scattered surface waves for these locations. We solve the inverse problem by using the interferometric traveltimes of the modeled scattered surface waves. The results show that the location of the scatterer is reasonably well estimated.

Introduction

Near-surface structures such as cavities, caves, tunnels, mineshafts, buried objects, archeological ruins, water reservoirs and similar, cause scattered surface waves. These near-surface scatterers may pose risk during and after the construction of buildings, transportation ways (roads, highways, railways) or power plants (wind, solar, etc) which are spread to wide areas. These scatterers can further be affected by the changes in the hydraulic regime, earthquakes and change of the loading on the soil and may thus pose hazards. Therefore, the detection and monitoring of this type of weak zones is important to mitigate environmental and geohazards.

Several authors used scattered surface waves for imaging cavities, buried objects, or shallow water reservoirs (Snieder, 1987; Herman et al, 2000; Campman and Riyanti, 2007; Kaslilar, 2007). The scattered surface waves are studied in detail in terms of seismic interferometry by Halliday and Curtis (2009). Recently Mikesell et al, (2012) explained how the correlation of coda waves can be exploited to locate individual scatterers.

In this study the correlation-type interferometric estimate of the ghost scattered surface waves is used for obtaining the location of a near-surface scatterer. Seismograms were produced by using finite difference modeling of elastic wave propagation (Thorbecke and Draganov, 2011). These seismograms are dominated by direct surface waves, which are unfavorable for the utilization of the scattered surface waves. To obtain a clear scattered surface wave, the method of interferometric prediction and subtraction of surface wave introduced by Dong et al (2006), is considered. The code given in Schuster (2009) is modified and used for this study. After removing the direct surface waves, the interferometric estimates of the ghost scattered wavefields are obtained for selected virtual-source locations. The traveltimes of the ghosts are picked and inverted by using the theoretical ghost traveltimes. The end results are the horizontal and vertical locations of the scatterer. To assess the inversion results, the data resolution, the model resolution and the model covariance matrices are calculated and the results are discussed.

It is anticipated that the introduced method will be more effective than other methods when lateral changes of the medium properties, such as velocity gradient or random inhomogeneties, are present. As seismic interferometry effectively redatums sources (or receivers) from places away from the scatterers to the target area, the unwanted extra effects, due to propagation from sources through the laterally changing medium and/or scatterers to the receivers close to the target area, are eliminated. Using the interferometric traveltimes of the ghosts the scatterers can be located. The method can also reduce the calculation times for waveform inversion studies. Although this study is initiated at geotechnical scale, the suggested method is not restricted to geotechnical studies. It can also be used in exploration and global seismology for detecting the near-surface scatterers.

Calculation of the Interferometric Ghost of the Scattered Surface Waves

In order to obtain a scattered wavefield, a series of seismograms were produced by the 2D finite difference wavefield modelling program of Thorbecke and Draganov, (2011). The geometry and the medium parameters of the models are given in Figure 1. A total of 81 shot gathers are obtained by shifting the source location closer to the scatterer by 0.5 meters. Figure 2 shows one of the shot gathers.

The code given in Schuster (2009) is modified for this study and the direct Rayleigh waves from the seismograms are eliminated by interferometric prediction (Figure 3). Seismic interferometry is applied to the now clear scattered waves by cross-correlating the reference trace d^{VS} (the trace at the virtual-source position) with the rest of the traces, d^i, which are present on the seismic record. This relation is

$$C_{d^i d^{VS}}(\tau) = \sum_t d_t^i d_{t+\tau}^{VS} . \quad (1)$$

Note that as the active source is at the surface while the scatterer is at depth, the source is not at the stationary phase region for retrieving a physical scattered surface waves. Application of equation (1) will eliminate the common travel path from the source to the scatterer and

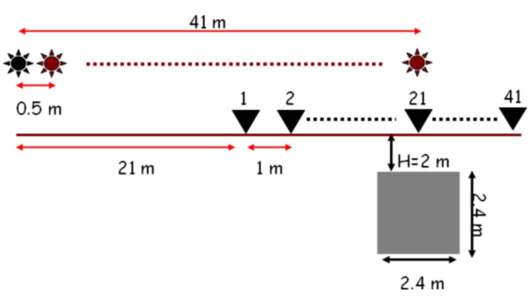

	Background	Scatterer
ρ (kg/m³)	1800	1000
V_p (m/s)	700	400
V_s (m/s)	400	170

Figure 1: Schematic view of the scale model (top): The sources (stars), receivers (triangles) and scatterer (grey square). The modelling parameters for the background and the scatterer are given on the table (below).

will result in the retrieval of a ghost scattered surface wave.

The modeled buried object scatters the illumination wavefield in the same way irrespective of the position of the surface source. For this reason, the retrieved ghost scattered surface waves will be the same for any position of the surface source, except for the case when losses are present in the medium. In the latter case, the only change in the retrieved ghost will be in its dominant frequency. In Figure 3b-d the retrieved ghost scattered surface waves for virtual-source locations at receivers 1, 21 and 30 are given respectively. It can be seen that the scattered fields are the same, but for a displacement along the time axis. This displacement depends on the distance from the virtual source to the scatterer only. Change in the lateral direction of the medium parameters to the left and to the right of the receiver array will not affect the retrieved ghost traveltimes. The picked traveltimes are shown by the red curves on Figure 3b-d. In the next section these traveltimes are used for obtaining the location of the scatterer.

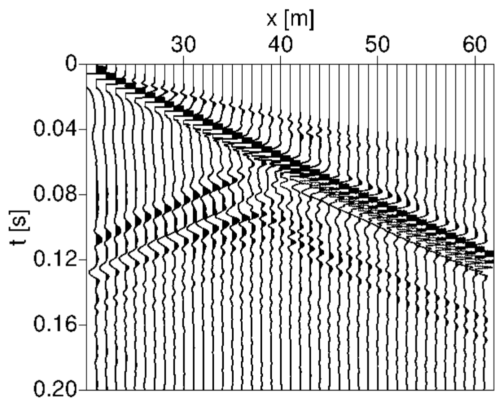

Figure 2: Shot gather generated with finite difference modelling.

Estimation of the Location of the Scatterer

To estimate the location of the scatterer, the following theoretical ghost travel time relation is used,

$$t = \frac{1}{V_R}\left\{\left[\left(x_i^r - x\right)^2 + \left(z_i^r - z\right)^2\right]^{1/2} - \left[\left(x_{vs} - x\right)^2 + \left(z_{vs} - z\right)^2\right]^{1/2}\right\} \tag{2}$$

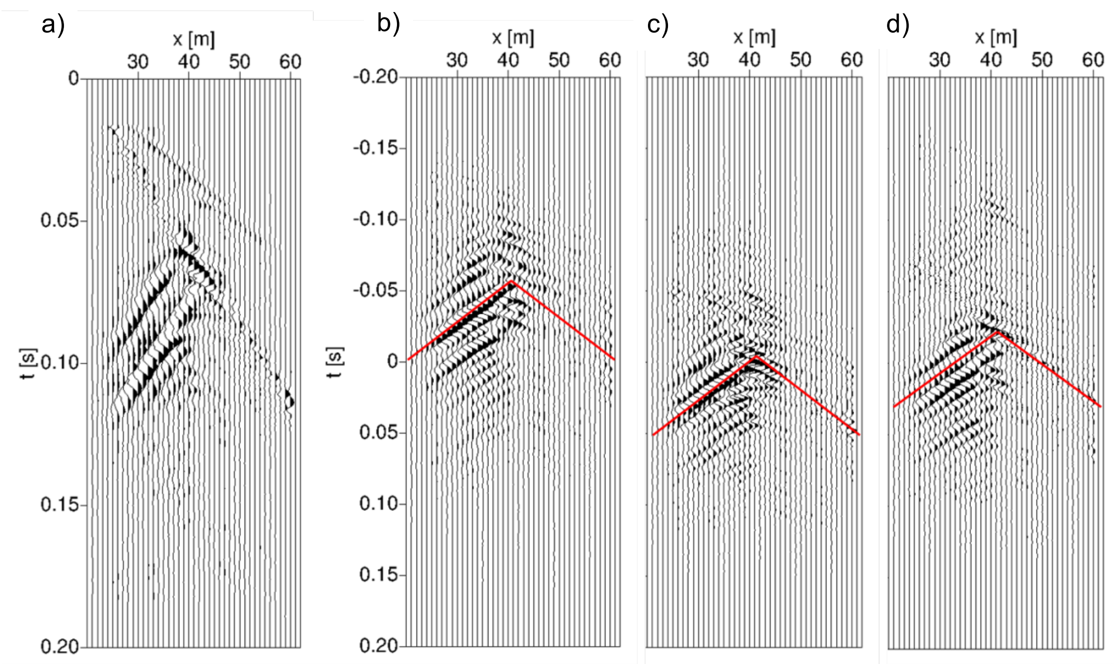

Figure 3: (a) The scattered wavefield, (b), (c) and (d): Ghost scattered surface waves retrieved by applying seismic interferometry to (a) for virtual source locations at receivers 1, 21 and 30, respectively. Figures are plotted by Seismic Un*x (Cohen and Stockwell, 2000)

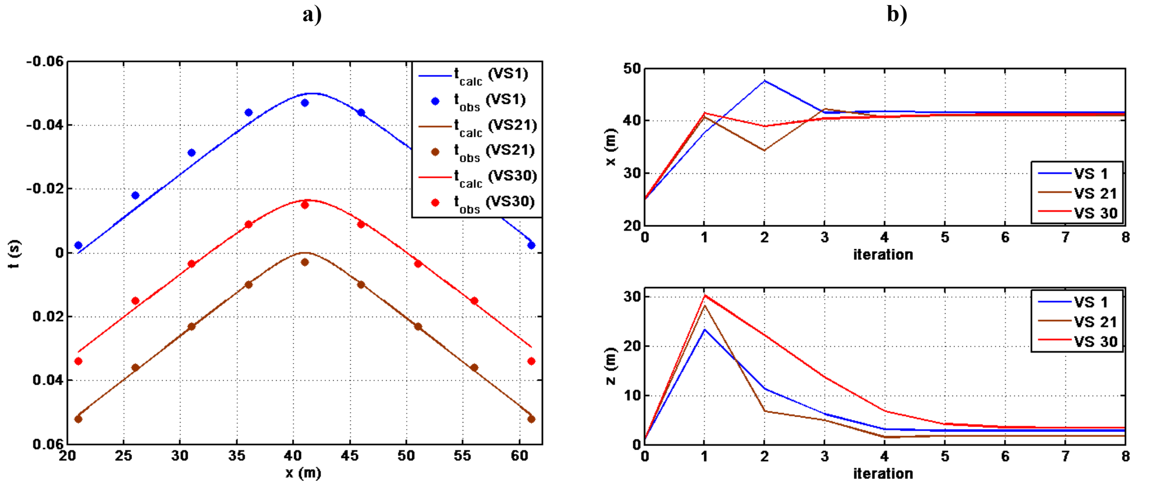

Figure 4: (a) The observed (dot) and the calculated (solid line) travel times, (b) estimated horizontal and vertical locations of the scatterer for the virtual sources 1 (blue), 21 (brown) and 30 (red).

The relation gives the retrieved ghost traveltimes between the virtual source, the scatterer and the receivers. In the equation, V_R is the Rayleigh wave velocity, i is the index for the receiver numbers, r and VS denote the receiver, and the virtual source, respectively, while x and z are the locations of the scatterer in the horizontal and vertical direction, respectively.

To find the location of the scatterer, the traveltime relation (equation 2) and the traveltimes obtained for each virtual source location (red curves in Figure 3b to d) are used in the inversion. The nonlinear problem is solved iteratively. The system of equations for the forward problem is denoted as $\Delta\mathbf{d} = \mathbf{G}\Delta\mathbf{m}$. In this relation, the difference between the observed t_{obs} (retrieved), and the calculated t_{calc} (equation 2) ghost scattered data is denoted by $\Delta\mathbf{d} = t_{obs} - t_{calc}$, the unknown model parameters - the horizontal x and vertical z locations of the scatterer are denoted by the vector $\Delta\mathbf{m}$, while the Jacobian matrix is represented by $\mathbf{G}$. The inverse problem is given in terms of damped Singular Value Decomposition (SVD) as,

$$\Delta\mathbf{m} = \mathbf{V}\boldsymbol{\Lambda}\left(\boldsymbol{\Lambda}^2 + \beta^2\mathbf{I}\right)^{-1}\mathbf{U}^T\Delta\mathbf{d}, \tag{3}$$

where $\mathbf{V}, \mathbf{U}, \boldsymbol{\Lambda}, \mathbf{I}$ and β are the model-space eigenvectors, the data-space eigenvectors, the diagonal matrix containing the eigenvalues, the identity matrix and the damping parameter, respectively. Considering equation (3), the inverse problem is solved to find the location of the scatterer. The damping parameter is determined by plotting $\|\Delta\mathbf{m}\|_2^2$ versus $\|\Delta\mathbf{d}\|_2^2$. The best fit between the observed and calculated traveltimes of the ghost scattered surface waves for virtual sources 1, 21 and 30 (21, 41, and 50 m) are given in Figure 4a and the estimated model parameters are given in Figure 4b. It can be seen that there is a good agreement between the observed and the calculated traveltimes of the ghost scattered surface waves. The initial and the updated model parameters for each iteration are given in Figure 4b. After five iterations, the model parameters, the horizontal and vertical location of the scatterer, become closer to the actual values. It is observed that the location of the scatterer is well estimated.

To assess the inversion results, the data resolution (**N**), the model resolution (**R**) and the model covariance (cov[**m**]) matrices including the damping parameter are calculated by using the following relations (Randall and Zandt, 2007) ,

$$\mathbf{N} = \frac{\mathbf{U}\boldsymbol{\Lambda}^2\mathbf{U}^T}{\boldsymbol{\Lambda}^2 + \beta^2\mathbf{I}}, \tag{4}$$

$$\mathbf{R} = \frac{\mathbf{V}\boldsymbol{\Lambda}^2\mathbf{V}^T}{\boldsymbol{\Lambda}^2 + \beta^2\mathbf{I}}, \tag{5}$$

$$\mathrm{cov}[\mathbf{m}] = \sigma^2\frac{\mathbf{V}\boldsymbol{\Lambda}^2\mathbf{V}^T}{\left(\boldsymbol{\Lambda}^2 + \beta^2\mathbf{I}\right)^2}. \tag{6}$$

The images of the resolution and covariance matrices are given in Figure 5. It is observed that for the three virtual source locations, the diagonal of the model resolution matrix (**R**) is close to identity matrix, which indicates very good resolution or estimation of the model parameters (x and z). Also the best data resolution can be achieved if the data resolution matrix is unity. Here the values of the data resolution matrix (**N**) are around the diagonal, however it is not the identity matrix. That means the predicted data are weighted averages of the observed data. For example the rows of the data resolution matrix **N** for VS1 (Figure 5b), weight the observed data $\mathrm{d}_{1\text{-}4}^{obs}$ with weights close to zero. The observed data at receivers 1-4 correspond to the shortest interferometric travel times. The predicted data d_5^{pre} is weighted with the highest weight of **N**(5,5) in the middle and has the largest effect on the data solution. This point is above the scatterer. Data between 6-9, $\mathrm{d}_{6\text{-}9}^{obs}$, are weighted with the rows 6-9 of the data resolution matrix. The data resolution matrix corresponding to VS21 has nearly zero values at the location of the scatterer. This point corresponds to the shortest interferometric travel time again. Similar results are also obtained for the VS41.

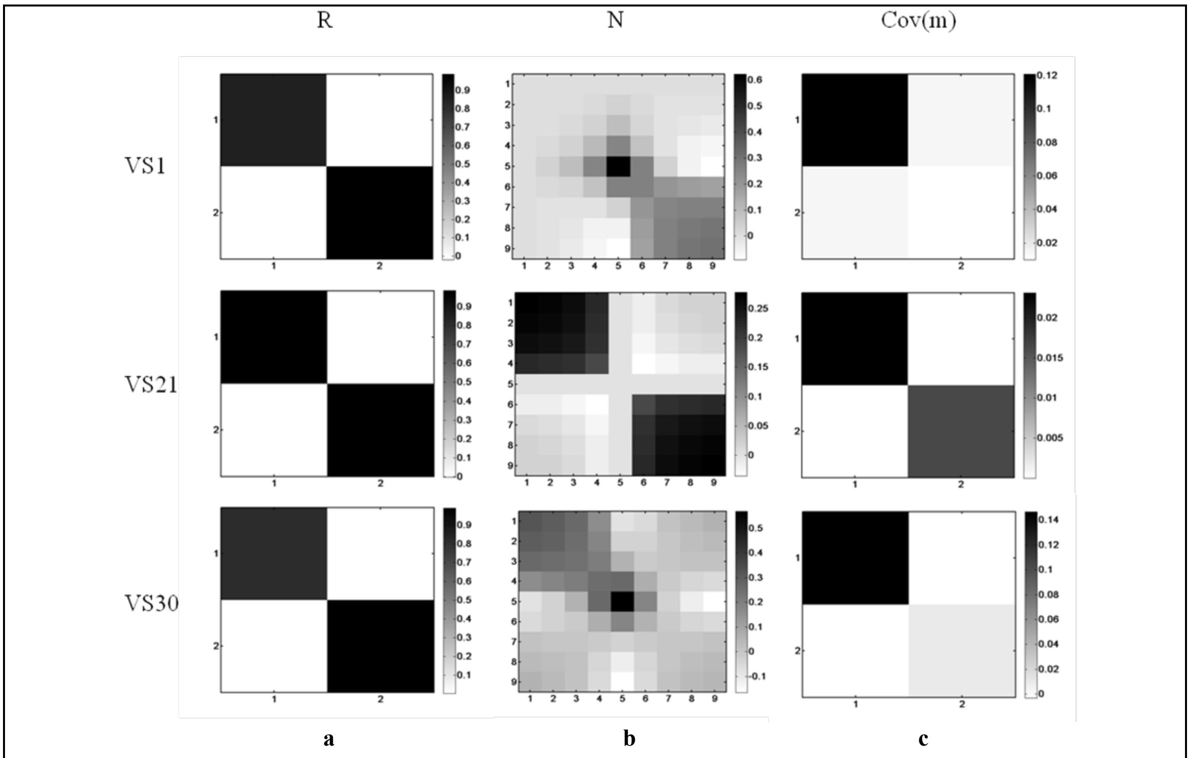

Figure 5: The model resolution, data resolution and model covariance matrices

The uncertainities in the model parameters for the virtual sources are obtained by calculating the model covariance matrices. The temporal sampling $\Delta t = 10^{-3}$s is selected as the standard deviation of the data errors and used in equation 6. For all virtual source positions, it is observed that the model parameters (x and z) are estimated with less than 4% uncertainty. And the errors in the estimated model parameters are less than 10 %.

Conclusions

A method for obtaining the location of a near-surface scatterer is proposed by using traveltimes of non-physical (ghost) scattered surface waves retrieved from seismic interferometry. The ghost scattered surface waves are obtained by cross-correlating the recorded scattered surface waves originating from only one source at the surface. The traveltimes of the ghost scattered surface waves are used in an inversion to find the location of the scatterer. The depth and the horizontal position of the scatterer are estimated for different virtual-source locations.

Acknowlegments

This work is supported by ***TUBITAK (The Scientific and Technological Research Council of Turkey)*** with the project ***110Y250*** titled "***Detecting Near-surface Scatterers by Inverse Scattering and Seismic Interferometry of Scattered Surface Waves***" and by ***Istanbul Technical University Research Fund***. We gratefully acknowledge this financial support.

REFERENCES

Campman, X. and Riyanti, C. D., 2007, Non-linear inversion of scattered seismic surface waves, *Geophys. J. Int.,* **171**, 1118-1125.

Dong, S., R. He, and G. T. Schuster, 2006, Interferometric prediction and least-squares subtraction of surface waves, 76th Annual International Meeting, SEG, Expanded Abstracts, 2783–6.

Halliday D.F., and Curtis, A., 2009, Seismic interferometry of scattered surface waves in attenuative media, Geophys. J. Int., **185**, 419-446

Herman, G.C., Milligan, P.A., Huggins, R.J. and Rector, J.W., 2000, Imaging shallow objects and heterogeneities with scattered guided waves, *Geophysics,* **65**, no. 1, 247-252.

Kaslilar, A., 2007, Inverse scattering of surface waves: imaging of near-surface heterogeneities. Geophys. J. Int., **171**, 352-367.

Mikesell, T.D., van Wijk, K., and Blum, T.R., 2012, Analyzing the coda from correlating scattered surface waves, **131**, J. Acoust. Soc. Am., issue 3, EL275-EL281.

Schuster, G. T., 2009, Seismic interferometry: Cambridge University Press, p138-141.

Snieder, R.K., 1987, Surface wave holography. *in* G.Nolet, ed., Seismic tomography: *D.Reidel Pub. Co.,* 323-337.

Thorbecke, J., and Draganov, D., 2011, Finite-difference modeling experiments for seismic interferometry Geophysics, **76**, no. 6, H1--H18, doi: 10.1190/GEO2010-0039.1

Randall, M.R. and Zandt, G. 2007, Inverse Problems in Geophysics, Lecture Notes, Dept. of Geosciences, University of Arizona, Tucson, Arizona 8521.